Fundamental mechanisms of ^{3}He relaxation on glass

R.E. Jacob [a,*], B. Driehuys [b], B. Saam [a]

[a] *University of Utah, 115 S. 1400 E., Salt Lake City, UT 84112, USA*
[b] *Amersham Health, 2500 Meridian Pkwy. Suite 150, Durham, NC 27713, USA*

Abstract

We present a model of ^{3}He relaxation on the surface of borosilicate glass which accurately predicts observed relaxation rates and their temperature dependence. Above room temperature ^{3}He dissolves into Pyrex, where interactions with Fe^{3+} ions result in a relaxation time of ≈ 1 ms. Gas exchange across the glass surface of an enclosed vessel leads to $T_1^{-1} = A/V(3.9 \pm 1.4) \times 10^{-2}$ cm/h at room temperature, where A/V is the surface-to-volume ratio. The activation energy for relaxation is 13.7 ± 0.7 kJ/mol and is dominated by the activation energy of ^{3}He diffusion in glass. This is the first successful confirmation of predicted ^{3}He relaxation rates in glass vessels.
© 2003 Elsevier Science B.V. All rights reserved.

1. Introduction

Spin-exchange optical pumping (SEOP) [1] and metastability-exchange optical pumping (MEOP) [2] are common methods of producing very high, non-equilibrium nuclear polarization in certain noble gas nuclei. The gas is typically polarized and/or stored in glass vessels, or cells. Workers in the field have long attempted to determine a quantitative and predictive model of ^{3}He surface relaxation on glass. Since ^{3}He surface relaxation has proven to be a very complex problem, understanding even a single-model system would be critical progress. The ultimate goal is a better understanding of ^{3}He relaxation in spin-exchange cells (cells containing an alkali metal), where magnetic inclusions in the glass can dominate relaxation [3]. Researchers who use bare glass cells of all types, and Pyrex in particular, as storage cells for polarized gas research may find these results especially pertinent.

Previous measurements of ^{3}He relaxation as a function of temperature on glass surfaces have been made in bare (containing no Rb or surface coatings), sealed Pyrex, aluminosilicate, and quartz cells [4,5]. For Pyrex, Fitzsimmons et al. provided significant insight into ^{3}He relaxation mechanisms by showing that adsorption dominates relaxation below about 130 K and absorption dominates at higher temperatures. They derived and verified a model for adsorption-based relaxation. However, a quantitative understanding of the absorption regime, which is relevant for most practical experiments, has eluded research-

---

ers. In this Letter, we provide a theory valid for all bare Pyrex cells which accurately predicts the measured rates for dissolution-dominated relaxation. We show that such relaxation can be characterized by an Arrhenius relation with a relaxivity ϱ_0 and the appropriate activation energy E_A

$$\frac{1}{T_1} = \frac{A}{V} \varrho_0 \exp\left(-\frac{E_A}{RT}\right), \tag{1}$$

where A/V is the surface to volume ratio.

2. Theory

2.1. T > room temperature

Our model for relaxation of polarized ^{3}He is based on the solubility, diffusivity, and intrinsic relaxation of ^{3}He in the glass. We assume that all relaxation is due to interactions of ^{3}He with paramagnetic impurities in the glass, and that the number of ^{3}He atoms in the gas is much greater than that of dissolved atoms. The net flow of magnetization is from the gas to the glass in the $-\xi$ direction, while $\xi = 0$ represents the glass–gas interface. In the limit of weakly relaxing walls [6], the polarization may be assumed uniform in the gas and continuous across the glass–gas interface.

The diffusion equation in the glass is

$$\frac{\partial}{\partial t} M(\xi) = D_b(T)\frac{\partial^2}{\partial \xi^2} M(\xi) + Q(\xi), \tag{2}$$

where $D_b(T)$ is the temperature-dependent diffusion coefficient of the helium in the bulk glass, $M(\xi)$ is the ^{3}He magnetization, and $Q(\xi)$ is a source term. The magnetization loss is

$$\frac{\partial}{\partial t} M(\xi) = -\frac{1}{T_1} M(\xi), \tag{3}$$

where T_1 is the measured relaxation time. The source term represents the magnetization destroyed while in the dissolved phase

$$Q(\xi) = -\frac{1}{T_{1b}(T)} M(\xi), \tag{4}$$

where $T_{1b}(T)$ is the temperature-dependent relaxation time of the dissolved gas. From the above assumptions, $T_1 \gg T_{1b}$. Eq. (2) becomes

$$D_b(T)\frac{\partial^2}{\partial \xi^2} M(\xi) - \frac{1}{T_{1b}(T)} M(\xi) \approx 0. \tag{5}$$

The general solution to Eq. (5) is

$$M(\xi) = S(T) M_0 \exp(\xi/\lambda), \tag{6}$$

where M_0 is the gas-phase magnetization, $S(T)$ is the Ostwald solubility (Suckow [7] refers to the Bunsen solubility, [1] which we will use in later calculations), and $\lambda = \sqrt{D_b(T)\,T_{1b}(T)}$ represents a characteristic penetration depth of magnetization in the glass. We note that solubility is usually calculated from measurements of permeability K and diffusivity, since $S = K/D$.

The observed rate I at which total magnetic moment leaves the gas phase and enters the dissolved phase is

$$I = -\frac{M_0 V}{T_1}, \tag{7}$$

where V is the cell volume. This rate is also the flux of total magnetic moment at the interface multiplied by the interface area A

$$I = -A D_b \frac{\partial}{\partial \xi} M(\xi) = -A\sqrt{\frac{D_b(T)}{T_{1b}(T)}} M_0 S(T). \tag{8}$$

Eqs. (7) and (8) give a prediction for the relaxation rate of polarized ^{3}He in a bare glass cell entirely in terms of the cell geometry and the bulk glass properties

$$\frac{1}{T_1} = \frac{A S(T)}{V}\sqrt{\frac{D_b(T)}{T_{1b}(T)}}. \tag{9}$$

A similar equation was partially derived by Deaton et al. [8] in their study of ^{3}He relaxation on polymer surfaces.

The general form of relaxation due to dipolar interactions in the bulk [9] is

$$\frac{1}{T_{1b}} = \frac{6}{15}\frac{\mathscr{M}}{r^6}\frac{\tau_c}{1 + \omega^2 \tau_c^2}, \tag{10}$$

where r is the separation, τ_c is the correlation time of the interaction, ω is the ^{3}He Larmor frequency,

---

[1] The Ostwald solubility is the volume of gas dissolved in a unit volume of a liquid at a specified temperature and pressure. Bunsen solubility is the Ostwald solubility measured at STP.

and $\mathscr{M} = \gamma_{gas}^2 \gamma_e^2 \hbar^2 \mathscr{S}(\mathscr{S}+1)$, where γ_{gas} and γ_e are the gyromagnetic ratios for ^{3}He and electrons, respectively. Mazitov et al. [10] show that ^{3}He relaxation in bulk borosilicate glass depends most strongly on interactions with Fe^{3+} ions (spin $\mathscr{S} = 5/2$), which have a correlation time τ_{Fe} for electron spin flips of approximately 8×10^{-9}s at room temperature. To consider the effect of all Fe^{3+} ions on a ^{3}He nucleus, the expression in Eq. (10) must be integrated from the distance of closest approach a through all space

$$\frac{1}{T_{1b}} = \int_a^\infty \frac{6}{15} \frac{\mathscr{M}}{r^6} \frac{\tau_c}{1+\omega^2\tau_c^2} N 4\pi r^2 \, dr, \qquad (11)$$

where N is the density of Fe^{3+} ions in the glass. Since $\tau_c \approx \tau_{Fe}$, Eq. (11) becomes

$$\frac{1}{T_{1b}} = \frac{24\pi}{45} \frac{N\mathscr{M}}{a^3} \frac{\tau_{Fe}}{1+\omega^2\tau_{Fe}^2}. \qquad (12)$$

Our measurements are made at low fields (see Section 3). Since $\omega^2\tau_{Fe}^2 \ll 1$ we can simplify Eq. (12) to

$$\frac{1}{T_{1b}} \approx \frac{24\pi}{45} \frac{N\mathscr{M}}{a^3} \tau_{Fe}. \qquad (13)$$

Combining Eqs. (9) and (13) gives

$$\frac{1}{T_1} = \frac{A}{V} \sqrt{\frac{24\pi}{45} \frac{N\mathscr{M}}{a^3}} S(T) \sqrt{\tau_{Fe}(T) D(T)}. \qquad (14)$$

The temperature dependence of $S(T)$, $D_b(T)$, and $\tau_{Fe}(T)$ can be characterized by Arrhenius relations [7,10]:

$$S(T) = S_0 \exp\left(-\frac{E_S}{RT}\right), \qquad (15)$$

$$D_b(T) = D_0 \exp\left(-\frac{E_D}{RT}\right), \qquad (16)$$

$$\tau_{Fe}(T) = \tau_0 \exp\left(-\frac{E_{Fe}}{RT}\right), \qquad (17)$$

where E_S, E_D, and E_{Fe} are molar activation energies for solubility, diffusion, and Fe^{3+} electron spin flips, respectively, R is the universal gas constant, and T is the absolute temperature. The subscript 0 indicates an asymptotic ($T \to \infty$) value. By substituting Eqs. (15)–(17) into Eq. (14) we have

$$\frac{1}{T_1} = \frac{A}{V} \sqrt{\frac{24\pi}{45} \frac{N\mathscr{M}}{a^3}} S_0 \sqrt{\tau_0 D_0} \exp\left(-\frac{E_A}{RT}\right)$$
$$= \frac{A}{V} \varrho_0 \exp\left(-\frac{E_A}{RT}\right), \qquad (18)$$

where we have defined ϱ_0 as the relaxivity and the total activation energy as

$$E_A = E_S + \frac{1}{2}(E_{Fe} + E_D). \qquad (19)$$

We are primarily interested in relaxation in Pyrex, a borosilicate glass made by Corning, because it is commonly used for spin-exchange cells. To calculate the relaxation rate predicted by Eq. (18) for Pyrex we use the values obtained from bulk glass measurements shown in Table 1. The τ_0 was calculated using Eq. (17) and values for E_{Fe} and τ_{Fe}. Based on [10] and a discussion with Mazitov, we assume a 10% uncertainty for τ_0 and N. As Shelby [11] points out, there is generally poor agreement in reported activation energies for permeation of He in Pyrex, ranging from 21.8 to 31.4 kJ/mol, and similar discrepancies exist for

Table 1
Important values for Eq. (18) for Pyrex glass

Variable	Value	Uncertainty	Units	Ref.
D_0	7.0×10^{-4}	0.6×10^{-4}	cm^2/s	[7]
E_D	27.8	0.5	kJ/mol	[7]
S_0	6.3×10^{-3}	0.6×10^{-3}	cm^3 STP/cm^3	[7]
E_S	1.5	0.6	kJ/mol	[7]
τ_{Fe} (295 K)	0.77×10^{-8}		s	[10]
τ_0	1.9×10^{-9}	10%	s	
E_{Fe}	-3.4	0.3	kJ/mol	[10]
N	8×10^{18}	10%	cm^{-3}	[10]
a	5		Å	[10]

diffusion measurements. Bulk-glass activation energies reported in [7] are used in Table 1 rather than measurements by several other workers (see e.g., [11–13]) because the former measurements were made on Duran, a borosilicate glass made by Schott which is very similar to Pyrex, and because an uncertainty was given with each of the measured values. From Eq. (13) we estimate the relaxation time in bulk glass as $T_{1b} \approx 1$ ms, therefore the magnetization penetration depth λ is ≈ 30 nm.

Inserting relevant values into Eq. (18) gives the relaxivity

$$\varrho_0 = (10 \pm 2) \text{ cm/h}. \tag{20}$$

Eq. (19) gives the activation energy

$$E_A = 13.7 \pm 0.7 \text{ kJ/mol}, \tag{21}$$

which is dominated by the activation energy of ^{3}He diffusion in glass. We then calculate an expected room temperature relaxation rate

$$\frac{1}{T_1} = \left[\frac{A}{V} (3.9 \pm 1.4) \times 10^{-2} \right] \text{ h}^{-1}. \tag{22}$$

Eq. (22) predicts that bare Pyrex is of marginal utility for polarized ^{3}He storage, a fact that has been verified by several investigators [5,14,15]. As discussed in Section 4.1, this situation changes drastically for cells containing alkali metals.

2.2. T < room temperature

At lower temperatures the ^{3}He lacks sufficient kinetic energy to overcome the potential barrier for dissolution. For example, 13.7 kJ/mol of kinetic energy is required for the ^{3}He to overcome the potential barrier of dissolution relaxation, whereas only 1.7 kJ/mol is available at 200 K. Relaxation mechanisms with negative activation energies, such as adsorption to the cell wall, will begin to dominate the measured T_1^{-1} as the temperature decreases. Although typical sticking times are only $\approx 10^{-13}$ s at room temperature [14], there is no potential barrier to overcome, since the interaction is slightly attractive. Fitzsimmons et al. [5] derive an expression for relaxation in a cell where adsorption dominates

$$T_1 = \frac{N}{n}(t_{ad} + T_{ad}), \tag{23}$$

where N is the total number of gas atoms in the cell, n is the total number of gas atoms adsorbed to the surface at any instant, t_{ad} is the average adsorbed-atom sticking time, and T_{ad} is the relaxation time of an adsorbed atom. The number of adsorbed atoms is assumed much less than N, and is given by $n = N\bar{v}A t_{ad}/(4V)$, where $\bar{v}$ is the mean thermal velocity of the ^{3}He atoms. They show that $T_{ad} \gg t_{ad}$ and that $T_{ad} = t_{ad}/2W$, where W is the probability of an adsorbed atom relaxing. The W is proportional to t_{ad}^2, and t_{ad} follows an Arrhenius relation with activation energy E_{ad}. Thus Eq. (23) becomes

$$\frac{1}{T_{1ad}} = \frac{A}{V} \kappa_0 \exp\left(-\frac{2E_{ad}}{RT} \right) \sqrt{T}, \tag{24}$$

where $\kappa_0 = W\sqrt{2R/N_A m\pi}$, the ^{3}He mass is m and N_A is Avogadro's number. Müller [16] reports an activation energy of He adsorption on glass of

$$E_{ad} = -0.96 \pm 0.19 \text{ kJ/mol}. \tag{25}$$

This was independently confirmed by Fitzsimmons et al. [5] by observing nuclear spin-relaxation of polarized ^{3}He in low-pressure, sealed cells at various temperatures below room temperature.

By assuming that a ^{3}He atom will only relax in a collision with a Fe^{3+} ion at the surface, we can approximate W and find κ_0. The Fe^{3+} concentration is about one part in 10^4 by volume [10], and Timsit et al. [14] estimate that the average number of collisions needed to relax a ^{3}He atom is 10^6. Therefore, $\kappa_0 \approx 3 \times 10^{-2}$ cm h^{-1} K$^{-1/2}$.

3. Experimental

All measurements were made on spherical, valved, bare Pyrex cells. Cells prepared at Utah were ≈ 50 cm^3 and contained ≈ 4 amagats of ^{3}He, and the cell prepared at Amersham Health (AH) was ≈ 180 cm^3 and contained ≈ 1 amagat of ^{3}He. The Utah cells were prepared by baking under vacuum for ≈ 48 h at up to 400 °C. (Procedures used at Utah for cell fabrication and a detailed description of the cells can be found in [17].) Polarized gas was transferred into an evacuated cell from a similar, higher pressure spin-exchange cell by connecting the cells, opening the valves, and

allowing the pressure to equilibrate. The gas could not be polarized in the cells directly because bare cells, as we define them, do not contain Rb. All Utah T_1^{-1} measurements were made at ≈ 30 G using 100 kHz pulse NMR [18] and very small flip angles to excite only a small fraction of the gas. The AH measurements were made at ≈ 7 G (24 kHz). The initial heights of the free-induction decays acquired at appropriate time intervals were fit to a single exponential to extract T_1^{-1}. Several T_1^{-1} measurements could be made on a single charge of gas with intervening changes in temperature. The above room temperature measurements were done in a forced air oven typically used for SEOP. The temperature was maintained to a few tenths of a degree by a resistive temperature detector and controller. The measurements below room temperature were done in an insulated cylinder connected to a liquid nitrogen dewar. The desired temperature was reached by boiling off the liquid nitrogen at a specific rate with submerged heating tape powered by a variable AC transformer. The temperature was monitored with a thermocouple and maintained to within a few degrees. In all cases the cell valve was kept at room temperature to prevent o-ring failure.

4. Results and discussion

4.1. T > room temperature

Relaxation rates of three bare Pyrex cells, labeled 19A, 19B, and PXX05, were measured at various temperatures between 298 and 473 K (see Fig. 1). By comparing the average curve fit results of the three cells to Eq. (18) we find that $E_A = 14.7 \pm 0.3$ kJ/mol and $\varrho_0 = (36 \pm 4)$ cm/h (represented by the solid line in Fig. 1). This equates to a room temperature relaxation rate of

$$\frac{1}{T_1} = \left[\frac{A}{V} (9.6 \pm 1.6) \times 10^{-2} \right] \text{h}^{-1}. \quad (26)$$

Our results are in excellent agreement with the predicted value of $E_A = (13.7 \pm 0.7)$ kJ/mol and in good agreement with $\varrho_0 = (10 \pm 2)$ cm/h (represented in Fig. 1 by the dashed line), providing strong evidence that the model represented by
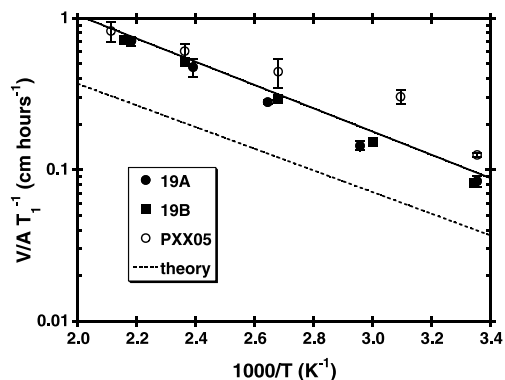

Fig. 1. $V/A \times T_1^{-1}$ vs $1000/T$ for three bare (no Rb) Pyrex cells. Eq. (18) is also plotted using Eqs. (20) and (21). Cells 19A and 19B were prepared and measured by the group at Utah, and cell PXX05 was prepared and measured at Amersham Health. Cells 19A and 19B were ≈ 50 cm^3 and ≈ 4 amagats, and cell PXX05 was ≈ 180 cm^3 and ≈ 1 amagat. Rates were measured at temperatures between 298 and 473 K. Bulk He–He relaxation was subtracted from the data. The data were fit to an Arrhenius relation with ϱ and E_A as free parameters. The resulting activation energy is $E_A = 14.7 \pm 0.3$ kJ/mol. Differences in the slopes represent a difference in E_A, whereas differences in the intercept could be due to an underestimation in A/V, since we assumed a smooth, spherical surface.

Eq. (18) accounts for the majority of relaxation in this temperature range. The discrepancy in the intercepts in Fig. 1 is directly related to the discrepancy in ϱ_0. We note, however, that the experimental value of ϱ_0 was obtained by assuming a perfectly smooth cell surface (minimum value of A/V). It is not difficult to imagine that the actual A/V is larger by a factor of 2 or more, which would bring the measured ϱ_0 into a much closer agreement with theory. In addition, slight differences in glass composition [19] or thermal history [20] could lead to variations in N or D_0 beyond the quoted errors we assumed. Differences in the relaxivity might also be due to additional or different relaxation mechanisms, although these would generally lead to non-linear behavior in Fig. 1 or to a slope different from that predicted. The theory accounts only for absorption relaxation, thus Eq. (22) represents a lower limit for T_1^{-1} at room temperature.

We have also studied the temperature-dependent relaxation of ^{3}He in several Pyrex cells containing Rb metal. In stark contrast to bare cells, we found that diffusion-based relaxation is absent

but that an adsorption-based relaxation model seems much more appropriate for the longest-lifetime cells. This suggests that the Rb strongly inhibits dissolution in spin-exchange cells leaving other relatively weak mechanisms to dominate relaxation. A detailed discussion of these results will be presented in a future publication.

4.2. T < room temperature

To investigate adsorption-based relaxation, we measured ^{3}He relaxation in a temperature range of 95 to 175 K. Fig. 2 shows T_1^{-1} vs $1000/T$ for two of the cells discussed in Section 4.1. Results of a global fit of the data to Eq. (24) give $E_{ad} = -0.63 \pm 0.03$ kJ/mol and $\kappa_0 = (1.6 \pm 0.1) \times 10^{-3}$ cm h^{-1} K$^{-1/2}$. There is good agreement between our value of κ_0 and the predicted value of 3×10^{-2} cm h^{-1}K$^{-1/2}$, although our value is somewhat lower. This could be a result of fewer Fe^{3+} ions on the glass surface than anticipated, and suggests the possibility of using polarized ^{3}He to measure Fe^{3+} ion surface concentration in various types of glasses. The activation energy we found was somewhat weaker (closer to zero) than that reported by Fitzsimmons et al. [5] and Müller [16] of -0.96 ± 0.19 kJ/mol.
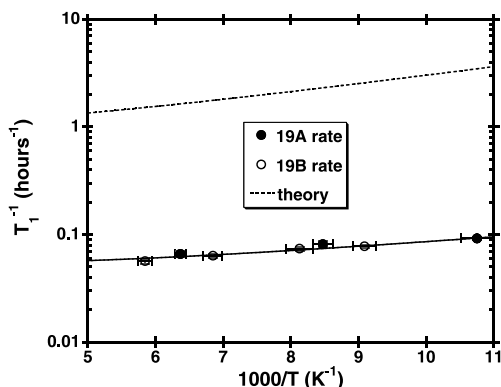
We note that Fitzsimmons et al. found a local minimum in T_1^{-1} of ^{3}He relaxation in bare Pyrex at about 120 K, reflecting the transition between adsorption- and absorption-dominated relaxation. We clearly observed adsorption behavior up to about 170 K and a local minimum at about 200 K. We have no direct explanation for the discrepancy, but we point out that the relevant data in [5] carry large error bars, particularly near the T_1^{-1} minimum; in addition the curves used to fit their data are at least somewhat speculative.

5. Conclusion

This work represents the first successful quantitative verification of predicted ^{3}He relaxation phenomena in bare Pyrex glass. We conclude that we have identified the correct relaxation mechanism for bare Pyrex, that our theoretical calculation represents a lower bound on T_1^{-1} and that experimental values will be larger as A/V departs from an ideally smooth surface. The relaxation is dominated by interactions of dissolved ^{3}He with Fe^{3+} ions in the glass. We have experimentally verified the predicted activation energy of dissolution-based relaxation, which depends on the activation energies of ^{3}He solution, diffusion, and Fe^{3+} electron spin flips. By comparing these results to the results of similar studies of vessels containing Rb, we will gain further insight in to the relaxation mechanisms in spin-exchange cells. This will lead to more consistent production of quality vessels and more efficient use of the spin-polarized gas.

Fig. 2. Relaxation rate vs $1000/T$ for two bare Pyrex cells at ≈ 4 amagats (two of the same cells shown in Fig. 1 but with a different charge of gas). The dashed line is a plot of Eq. (24) using Eq. (25) and κ_0. Temperatures ranged from about 95 to 175 K. The data, with bulk He–He relaxation subtracted, were fit to Eq. (24). The results from a global fit give an activation energy of $E_{ad} = -0.63 \pm 0.03$ kJ/mol, somewhat weaker than that reported in [5,16] of -0.96 ± 0.19 kJ/mol.

References

[1] T.G. Walker, W. Happer, Rev. Mod. Phys. 69 (1997) 629.
[2] T.R. Gentile, R.D. McKeown, Phys. Rev. A 47 (1993) 456.

[3] R.E. Jacob, S.W. Morgan, B. Saam, J.C. Leawoods, Phys. Rev. Lett. 87 (2001) 143004.

[4] J.G. Ganière, Helv. Phys. Acta 46 (1973) 147.

[5] W.A. Fitzsimmons, L.L. Tankersley, G.K. Walters, Phys. Rev. 179 (1969) 156.

[6] M.A. Bouchiat, J. Brossel, Phys. Rev. 147 (1966) 41.

[7] A. Suckow, P. Schlosser, H. Rup, R. Bayer, Glass Technol. 31 (1990) 160.

[8] D.M. Deaton, P.A. Cella, K.C. Hasson, D. Zollinger, B. Driehuys, Containers for hyperpolarized gas and associated methods, US Patent 6,128,918 (2000).

[9] N. Bloembergen, E.M. Purcell, R.V. Pound, Phys. Rev. 73 (1948) 679.

[10] R. Mazitov, P. Diehl, R. Seydoux, Chem. Phys. Lett. 210 (1993) 543.

[11] J.E. Shelby, J. Appl. Phys. 45 (1974) 2146.

[12] V.O. Altemose, J. Appl. Phys. 32 (1961) 1309.

[13] F.J. Norton, J. Am. Ceram. Soc. 36 (1953) 90.

[14] R.S. Timsit, J.M. Daniels, A.D. May, Can. J. Phys. 49 (1971) 560.

[15] W. Heil, H. Humblot, E. Otten, M. Schafer, R. Sarkau, M. Leduc, Phys. Lett. A 201 (1995) 337.

[16] D. Müller, Z. Phys. 188 (1965) 326.

[17] R.E. Jacob, S.W. Morgan, B. Saam, J. Appl. Phys. 92 (2002) 1588.

[18] B. Saam, M. Conradi, J. Magn. Reson. 134 (1998) 67.

[19] V.O. Altemose, J. Am. Ceram. Soc. 56 (1973) 1.

[20] L.C. Walters, J. Am. Ceram. Soc. 53 (1970) 288.